Electronic Supplementary Information for

Organometallic Copper(II) Complex of *meso-meso* N-Methyl N-Confused Pyrrole-Bridged Doubly N-Methyl N-Confused Hexaphyrin

Manik Jana,[a] Daniel Blasco,[b] Dage Sundholm*[c] and Harapriya Rath*[a]

a. School of Chemical Sciences, Indian Association for the Cultivation of Science, 2A/2B Raja S.C Mullick Road, Jadavpur, Kolkata, West Bengal 700 032, India. ichr@iacs.res.in

b. Departamento de Química, Instituto de Investigación en Química (IQUR), Universidad de La Rioja, Madre de Dios 53, 26006, Logroño, Spain.

c. Department of Chemistry, Faculty of Science, University of Helsinki, P. O. Box 55 (A. I. Virtasen aukio 1), FIN-00014, Helsinki, Finland. sundholm@chem.helsinki.fi

Table of Contents

Materials and Methods	S2-S4
General Synthetic Procedure	S4-S6
Spectroscopic Data	S7-S14
Calculations	S15-S24
Cartesian Coordinates	S25-S26

Materials and Methods:

1.1 Electronic absorption spectra were measured with a Perkin Elmer Lambda 950 UV-visible-NIR spectrophotometer. ^{1}H and ^{13}C NMR spectra were recorded on a spectrometer (operating at 300.132/400.20/500.13/600.13 MHz for ^{1}H and 75.47/100.64/125.77/150.05 MHz for ^{13}C) using the residual solvents as the internal references for ^{1}H [($CHCl_3$ (δ = 7.26 ppm), CH_2Cl_2 (δ = 5.32 ppm). Structural assignments were made with additional information from gCOSY, and gHSQC experiments. ESI HR-MS data were recorded using Waters QTOF Micro YA263 spectrometer. All solvents and chemicals were of reagent grade quality, obtained commercially and used without further purification except as noted. For spectral measurements, anhydrous dichloromethane was obtained by refluxing and distillation over CaH_2. Dry THF was obtained by refluxing and distillation over pressed Sodium metal. Thin layer chromatography (TLC) was carried out on alumina sheets coated with silica gel 60 F254 (Merck 5554) and gravity column chromatography were performed using Merck Silica Gel 230-400 mesh. Aluminum Oxide (Basic) grade II was purchased from Sigma Aldrich.

1.2 EPR Spectra of Copper complex 6

The electronic ground state of the Cu (II) complex is $^{2}B_1$ with configuration $(b2)^2\ (e)^4\ (a1)^2\ (b1)$. [b1; $d_{x^2-y^2}$, a; d_{z^2}, e; d_{xz}, d_{yz}, b2; d_{xy}] The ESR spectrum of the frozen solution consists of two sets of metal hyperfine lines corresponding to the $g_{||}$ and $g_{\perp}$ tensors. The metal hyperfine lines are further split by the super hyperfine interactions with nitrogen of pyrrole rings. Two of the four copper parallel lines with the nitrogen super hyperfine structure are well resolved in low field to permit the calculation of $g_{||}$, $A_{||}^{Cu}$ and $A_{||}^{N}$. The third component of copper parallel line is merged with much stronger perpendicular lines to different extent while the fourth copper parallel line is invariably completely overlapped. The $g_{||}$ values in the present study were calculated by measuring the field at the midpoint between the second and third (M_I = 1/2 and -1/2) copper parallel lines. In the high field region of the spectrum (perpendicular region) there are 18 lines which are almost equally separated by ~ 16 gauss. The value of $g_{\perp}$ was calculated by measuring the magnetic field at the 8^{th} line of these 18 lines pattern. The bonding parameter (α^2) which is a measure of covalency of the in plane σ-bonding of the Cu-N bond was calculated using an expression[S1] based on the copper hyperfine tensor $A_{||}$ as

$\alpha^2 = -[(A_{||} /p) + (g_{||} - 2) + 3/7(g_{\perp} - 2) + C]$ where C is a constant.

1.3 Theoretical Calculation

The electronic structure calculations were carried out with TURBOMOLE v7.7.1.[S2] The magnetically induced current (MIC) density calculations were carried out with GIMIC.[S3-S6]

The structures were visualized and rendered with UCSF ChimeraX v1.6.[S7] The MIC streamline plots were visualized and rendered with ParaView v5.11.0.[S8] The molecular structures were optimized without geometrical constraints at the density functional theory (DFT) level[S9] with the CAM-B3LYP functional,[S10] the def2-TZVP basis sets on all atoms,[S11] and the D4 correction by Grimme to dispersion effects.[S12,S13] The resolution-of-the-identity (RI) approximation was employed throughout to accelerate the calculations.[S14-S16] The optimized structure of **5** was verified to be a minimum in the potential energy hypersurface by computing the vibrational frequencies analytically.[S17] The molecular structure of **6** was also optimized at the RI-DFT/CAM-B3LYP-D4 level with the def2-SVP basis sets.[S11,S16] The vibrational frequencies were calculated for the structure optimized with the smaller basis set because the calculations of vibrational frequencies on the open-shell molecule at the CAM-B3LYP-D4/def2-TZVP level were computationally expensive. All vibrational frequencies were real at the CAM-B3LYP-D4/def2-SVP level. The molecular structures obtained with the two basis sets are qualitatively the same (Fig. S16, RMSD of 0.08 Å) suggesting that the CAM-B3LYP-D4/def2-TZVP optimized structure is also a minimum.

The first twenty singlet-to-singlet vertical excitations were calculated at the time-dependent DFT (TD-DFT) level[S18-S20] with the CAM-B3LYP functional and def2-TZVP basis sets on all atoms. The MIC strengths were calculated with GIMIC at the CAM-B3LYP/def2-TZVP level of theory. The *g*-tensor components were calculated for **6** at the RI-DFT/CAM-B3LYP/x2c-TZVPall-2c level of theory[S10,S21] using the exact two-component (X2C) relativistic approach to account for relativistic and spin-orbit effects.[S22,S23]

References:

S1 (a) D. Kievelson and R. Neiman, *J. Chem. Phys.,* 1961, **35**, 149-155; (b) D. Kievelson and S. K. Lee, *J. Chem. Phys.,* 1964, **41**, 1896-1903.

S2 S. G. Balasubramani, G. P. Chen, S. Coriani, M. Diedenhofen, M. S. Frank, Y. J. Franzke, F. Furche, R. Grotjahn, M. E. Harding, C. Hättig, A. Hellweg, B. Helmich-Paris, C. Holzer, U. Huniar, M. Kaupp, A. Marefat Khah, S. Karbalaei Khani, T. Müller, F. Mack, B. D. Nguyen, S. M. Parker, E. Perlt, D. Rappoport, K. Reiter, S. Roy, M. Rückert, G. Schmitz, M. Sierka, E. Tapavicza, D. P. Tew, C. van Wüllen, V. K. Voora, F. Weigend, A. Wodyński and J. M. Yu, *J. Chem. Phys.,* 2020, **152**, 184107.

S3 J. Jusélius, D. Sundholm and J. Gauss, *J. Chem. Phys.,* 2004, **121**, 3952–3963.

S4 H. Fliegl, S. Taubert, O. Lehtonen and D. Sundholm, *Phys. Chem. Chem. Phys.,* 2011, **13**, 20500–20518.

S5 D. Sundholm, H. Fliegl and R. J. F. Berger, *WIREs Comput. Mol. Sci.,* 2016, **6**, 639–678.

S6 D. Sundholm, M. Dimitrova and R. J. F. Berger, *Chem. Commun.,* 2021, **57**, 12362–12378.

S7 E. F. Pettersen, T. D. Goddard, C. C. Huang, E. C. Meng, G. S. Couch, T. I. Croll, J. H. Morris and T. E. Ferrin, *Prot. Sci.,* 2021, **30**, 70–82.

S8 J. Ahrens, B. Geveci and C. Law, Para View: An End-User Tool for Large Data Visualization. Visualization Handbook, Elsevier, 2005.
S9 O. Treutler and R. Ahlrichs, *J. Chem. Phys.,* 1995, **102**, 346–354.
S10 T. Yanai, D. P. Tew and N. C. Handy, *Chem. Phys. Lett.,* 2004, **393**, 51–57.
S11 F. Weigend and R. Ahlrichs, *Phys. Chem. Chem. Phys.,* 2005, **7**, 3297–3305.
S12 E. Caldeweyher, C. Bannwarth and S. Grimme, *J. Chem. Phys.,* 2017, **147**, 034112.
S13 E. Caldeweyher, S. Ehlert, A. Hansen, H. Neugebauer, S. Spicher, C. Bannwarth and S. Grimme, *J. Chem. Phys.,* 2019, **150**, 154122.
S14 K. Eichkorn, O. Treutler, H. Öhm, M. Häser and R. Ahlrichs, *Chem. Phys. Lett.,* 1995, **240**, 283–290.
S15 K. Eichkorn, F. Weigend, O. Treutler and R. Ahlrichs, *Theor. Chem. Acc.,* 1997, **97**, 119–124.
S16 F. Weigend, *Phys. Chem. Chem. Phys.,* 2006, **8**, 1057–1065.
S17 P. Deglmann, K. May, F. Furche and R. Ahlrichs, *Chem. Phys. Lett.,* 2004, **384**, 103–107.
S18 R. Bauernschmitt and R. Ahlrichs, *Chem. Phys. Lett.,* 1996, **256**, 454–464.
S19 R. Bauernschmitt, M. Häser, O. Treutler and R. Ahlrichs, *Chem. Phys. Lett.,* 1997, **264**, 573–578.
S20 F. Furche and D. Rappoport, Density Functional Methods for Excited States: Equilibrium Structure and Electronic Spectra. In Computational Photochemistry, M. Olivucci, Ed. Elsevier: Amsterdam, 2005.
S21 Y. J. Franzke, R. Tress, T. M. Pazdera and F. Weigend, *Phys. Chem. Chem. Phys.,* 2019, **21**, 16658–16664.
S22 Y. J. Franzke and J. M. Yu, *J. Chem. Theory Comput.,* 2022, **18**, 2246–2266.
S23 Y. J. Franzke and J. M. Yu, *J. Chem. Theory Comput.,* 2022, **18**, 323–343.
S24 N. Halder, M. Sangeetha, D. Usharani and H. Rath, *J. Org. Chem.,* 2020, **85**, 2059−2067.
S25 T. D. Lash and A. L. Von Ruden, *J. Org. Chem.,* 2008, **73**, 9417–9425.

General Synthetic Procedure:

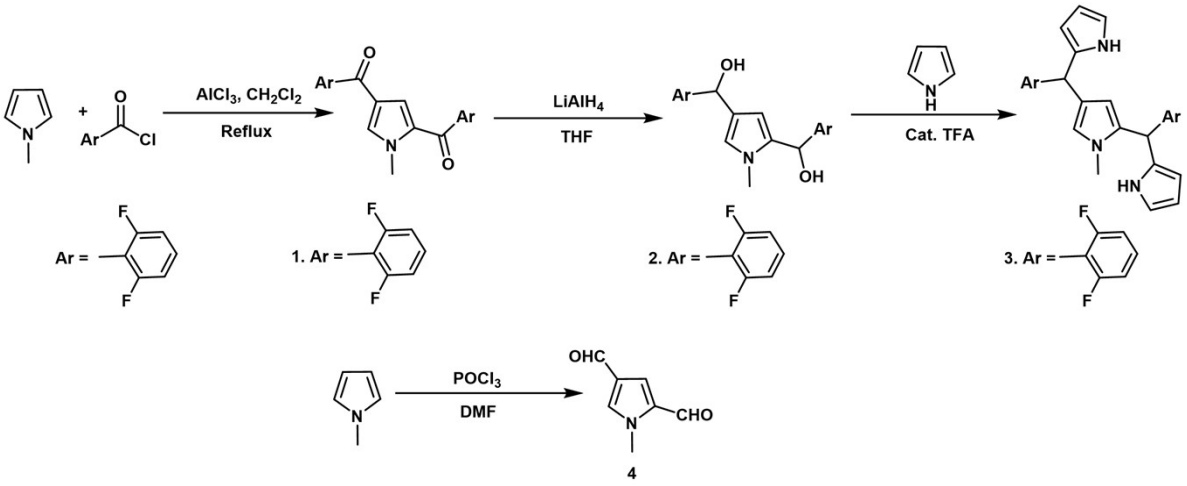

Scheme S1. Synthesis of all precursors used for the macrocycles reported in the manuscript[S24, S25]

Synthesis of **4** [S25]: Initially DMF (0.862 ml, 11.13 mmol) was taken in a three-neck round bottom flask under N_2. Then $POCl_3$ (1.21 ml, 12.95 mmol) was added dropwise into the

round bottom flask. After 15 min room temperature stirring reaction flask was placed in a 60° bath and kept for one hour. Then N-methyl pyrrole (0.5 ml, 5.63 mmol) was added dropwise into the reaction flask at room temperature and finally reaction mixture was stirred at 60° for an additional hour. Ice cold water was used to quench the reaction and then neutralized the reaction mixture by adding NaOAc. Organic layer was extracted with ether, washed with distilled water and dried over Na_2SO_4. After removing the solvent, the crude product was purified by flash Column chromatography purification using ethyl acetate/hexane as eluent to give light yellow solid as the final product.

[**4**] Yield. 280 mg (35%). M. P.: 95°C, HRMS (ESI-TOF) m/z: Calcd for $C_7H_7NO_2$ $[M]^+$, 137.0477; Found, 137.1393. ^{1}H NMR ($CDCl_3$, 300 MHz): δ 9.80 (s, 1H), 9.65 (s, 1H), 7.47 (s, 1H), 7.35 (s, 1H), 4.01 (s, 3H). ^{13}C {^{1}H} NMR ($CDCl_3$, 75 MHz) δ 184.90, 180.65, 135.46, 133.33, 125.97, 123.19, 37.60.

Synthesis of **5**: Tripyrrane **3** (0.463 g, 1 mmol) and N-methyl pyrrole-2, 4-dicarbaldehyde **4** (0.137 g, 1 mmol) were taken in a round bottom flask, to it 740 mL of dry DCM was added and stirred for 15 minutes under nitrogen atmosphere to get a clear solution. After that CF_3COOH (0.384 ml, 5.0 mmol) was added to the reaction mixture and stirred for 90 minutes under dark condition. The reaction mixture was then neutralized with triethylamine (0.348 ml, 2.5 mmol). After that, into the reaction mixture DDQ (566 mg, 2.5 mmol) was added and the resulting mixture was stirred at room temperature for another 90 minutes in open air. After complete removal of the solvent from the crude mixture by rotary evaporator, the compound was purified using basic alumina grade III where a blue colour band was eluted using 80% CH_2Cl_2/Hexane as eluent. These blue fractions collected from chromatography purification was evaporated and was further purified by repeated PTLCs. Recrystallized from CH_2Cl_2/Hexane yielding **5** as blue solid.

[**5**] Yield. 140 mg (13%). Mp > 350°C, HRMS (ESI-TOF) m/z: Calcd for $C_{61}H_{34}F_8N_7O_4$ $[M+H]^+$ 1080.2545; Found, 1080.2544. UV-vis (CH_2Cl_2, λ [nm], (ϵ [$M^{-1}cm^{-1}$ x 10^4]), 298K): 554 (3.65). ^{1}H NMR (CD_2Cl_2, 500 MHz): *δ* 13.34 (s, 1H), 11.43 (s, 1H), 8.31 (d, *J* = 5.0 Hz, 1H), 8.01 (d, *J* = 5.0 Hz, 1H), 7.90 (d, *J* = 5.0 Hz, 1H), 7.74 (m, 2H), 7.62 (d, *J* = 5.0 Hz, 1H), 7.55 (m, 2H), 7.40 (t, *J* = 8.5 Hz, 2H), 7.33 (t, *J* = 8.5 Hz, 2H), 7.23 (t, *J* = 8.5 Hz, 2H), 7.16 (t, *J* = 8.5 Hz, 2H), 7.06 (d, *J* = 5.0 Hz, 1H), 6.96 (d, *J* = 5.0 Hz, 1H), 6.62 (s, 1H), 6.54 (d, *J* = 5.0 Hz, 1H), 6.40 (d, *J* = 5.0 Hz, 1H), 5.95 (s, 1H), 2.87 (s, 3H), 2.64 (s, 6H). ^{13}C {^{1}H} NMR (CD_2Cl_2, 125 MHz): *δ* 171.92, 169.37, 162.71, 162.43, 162.41, 162.22, 162.10, 161.08, 160.82, 160.78, 160.60, 160.58, 160.51, 160.46, 148.80, 145.92, 145.71, 139.17, 137.78, 132.15, 131.96, 131.24, 130.03, 129.06, 128.29, 127.06, 126.76,125.35, 124.58, 121.42, 117.60, 117.33,116.85, 116.66, 116.54, 116.41, 115.36, 114.33, 112.87, 111.78, 111.64, 111.53, 111.36, 111.23, 104.05, 100.39, 92.75, 33.29, 28.32.

Synthesis of **6**: Macrocycle **5** (10mg, 0.00924 mmol) and $Cu(OAc)_2$ (16.78 mg, 0.0924 mmol) were taken in a three-neck round bottom flask. Then 10 mL dry THF was added into the reaction flask under N_2. After refluxing for 8 hours at 66ºC, the solvent was evaporated and compound **6** was separated by column chromatography using neutral alumina with 10% ethyl acetate/CH_2Cl_2 and finally recrystallized from CH_2Cl_2/Hexane yielding **5** as green solid.

[**6**] Yield. 13 mg (81%). Mp > 350°C, HRMS (ESI-TOF) m/z: Calc. for $C_{61}H_{31}CuF_8N_7O_4$ $[M]^+$ 1140.1606; Found, 1140.1608. UV-vis (CH_2Cl_2, λ [nm], (ϵ [$M^{-1}cm^{-1}$ x 10^4]), 298K): 402 (6.29), 615 (3.28), 709 (2.81).

Supplementary Data:

3.1 Mass Spectra

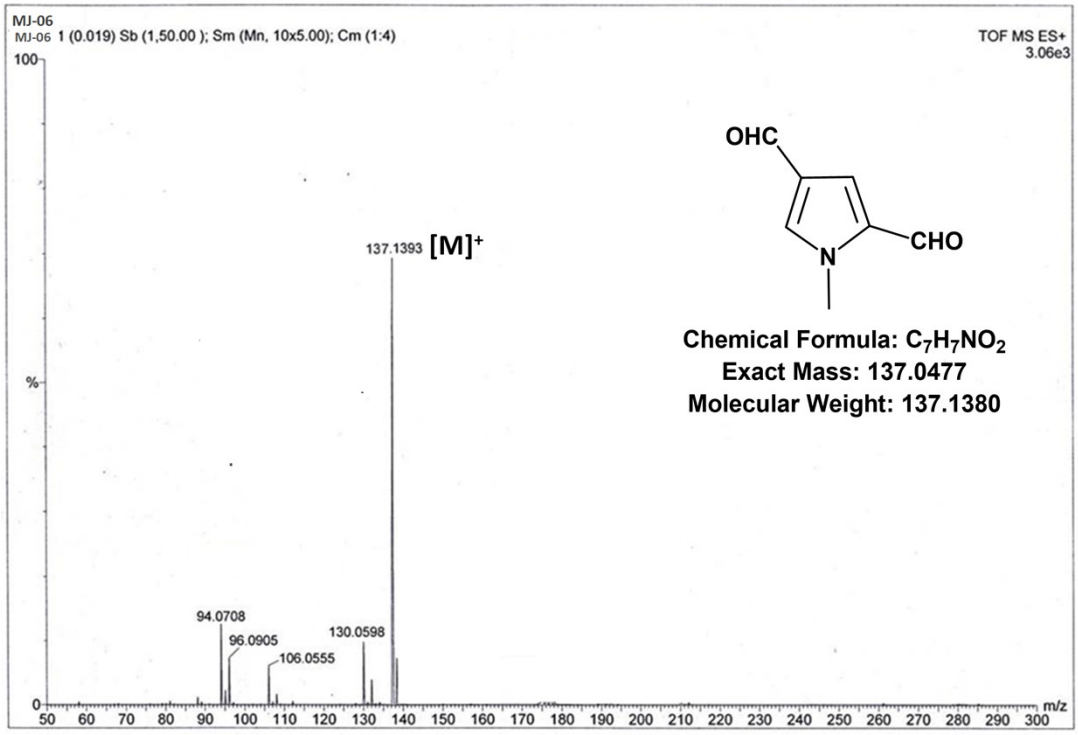

Fig. S1 HRMS Spectra of **4**.

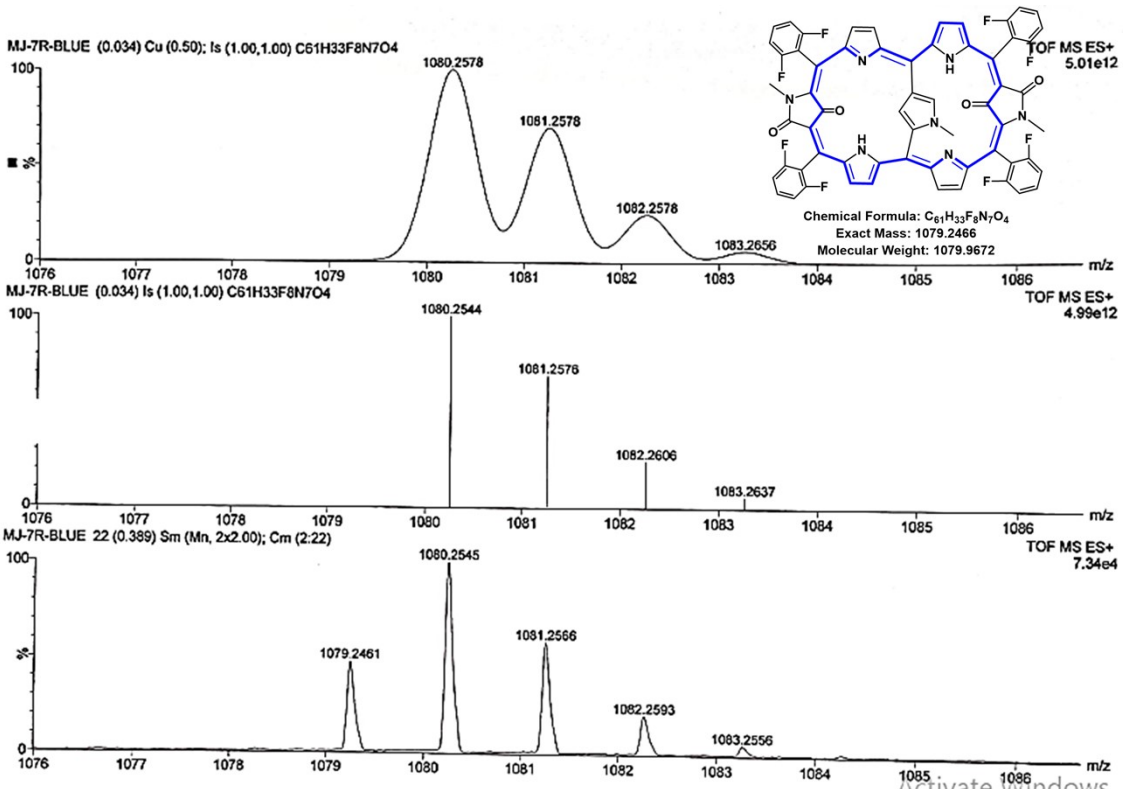

Fig. S2 HRMS Spectra of **5**.

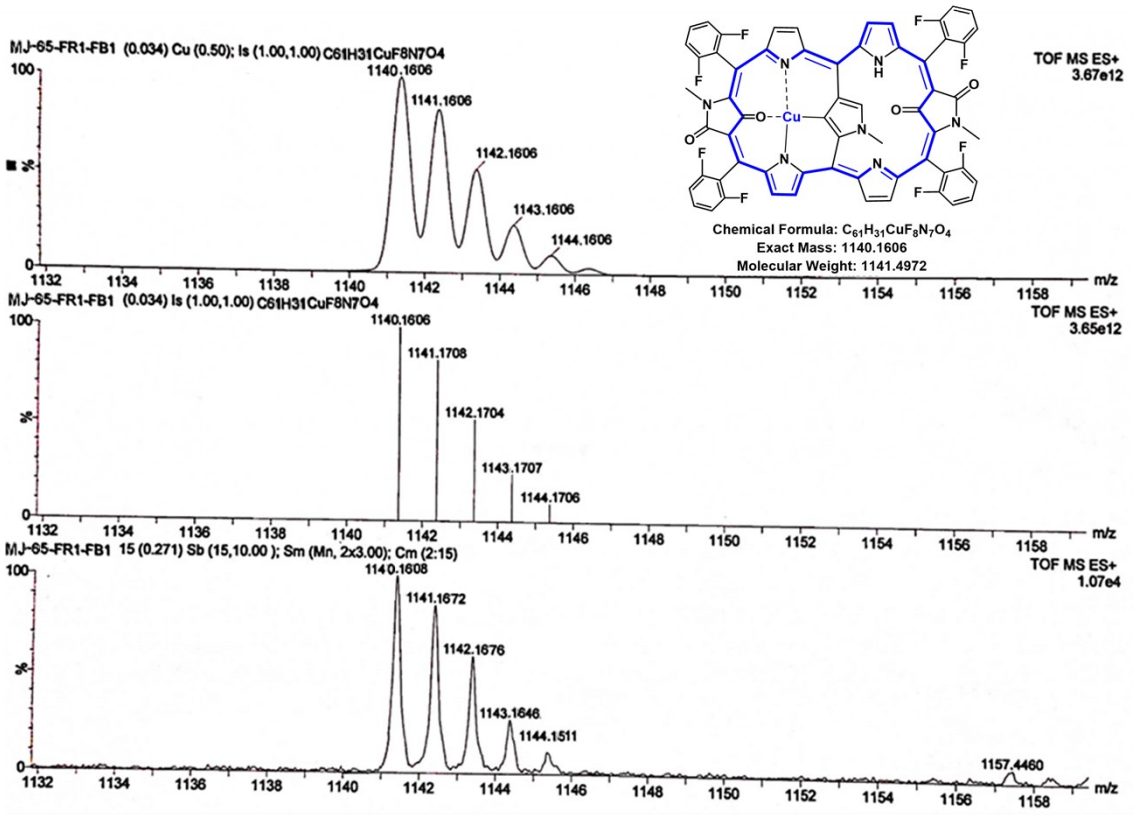

Fig. S3 HRMS Spectra of **6**.

3.2 IR spectra:

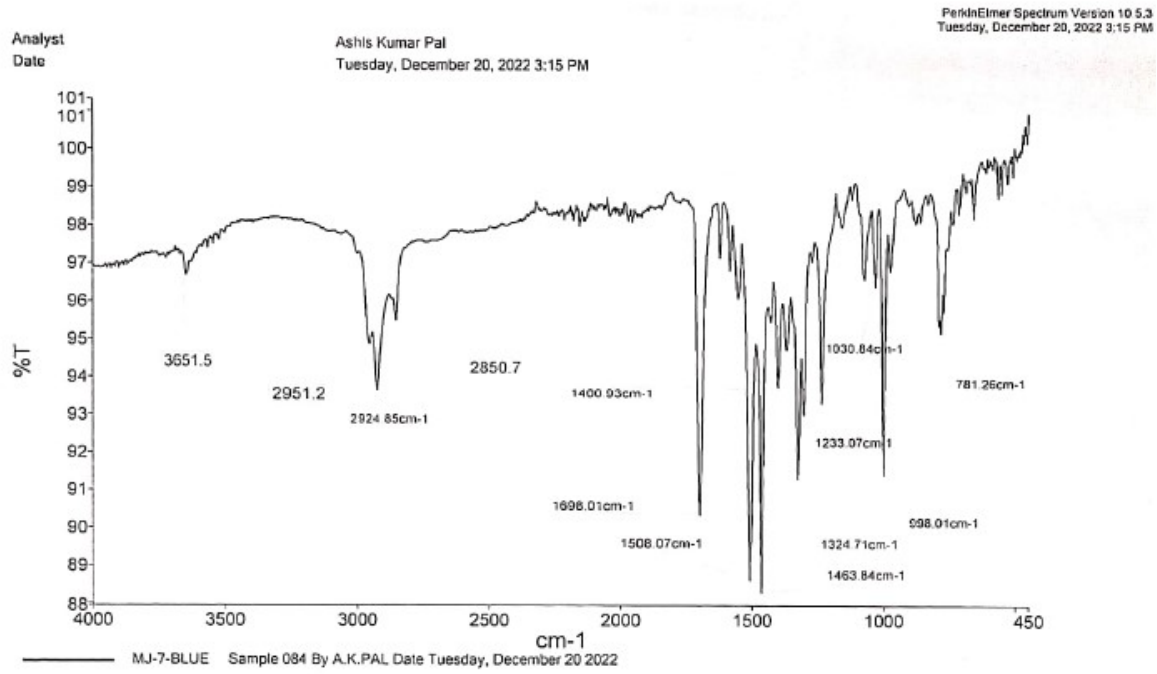

Fig. S4 IR Spectra of **5**

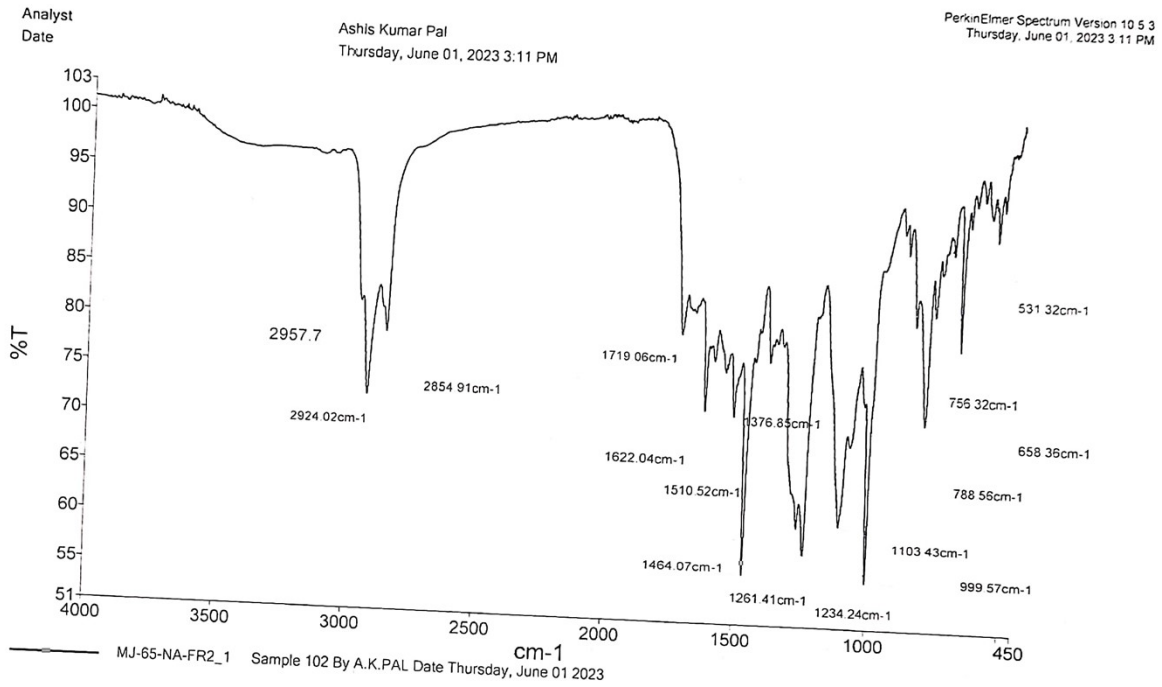

Fig. S5 IR Spectra of **6**

3.3 UV-vis spectra:

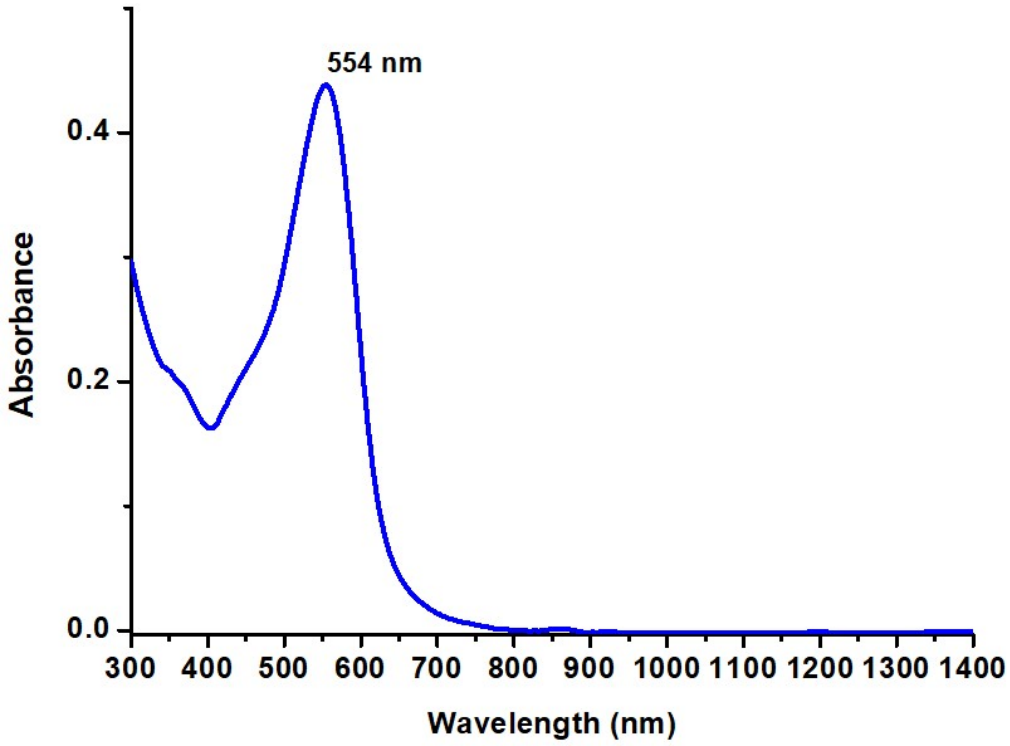

Fig. S6 UV-vis Spectra of **5**.

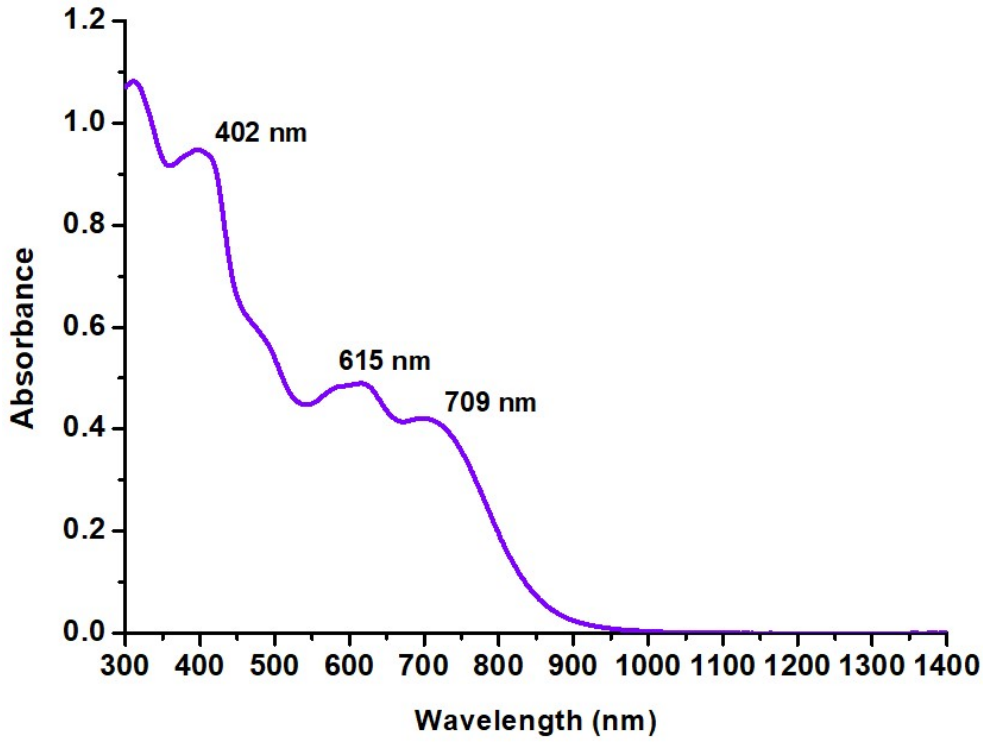

Fig. S7 UV-vis Spectra of **6**.

.

3.4 NMR spectra:

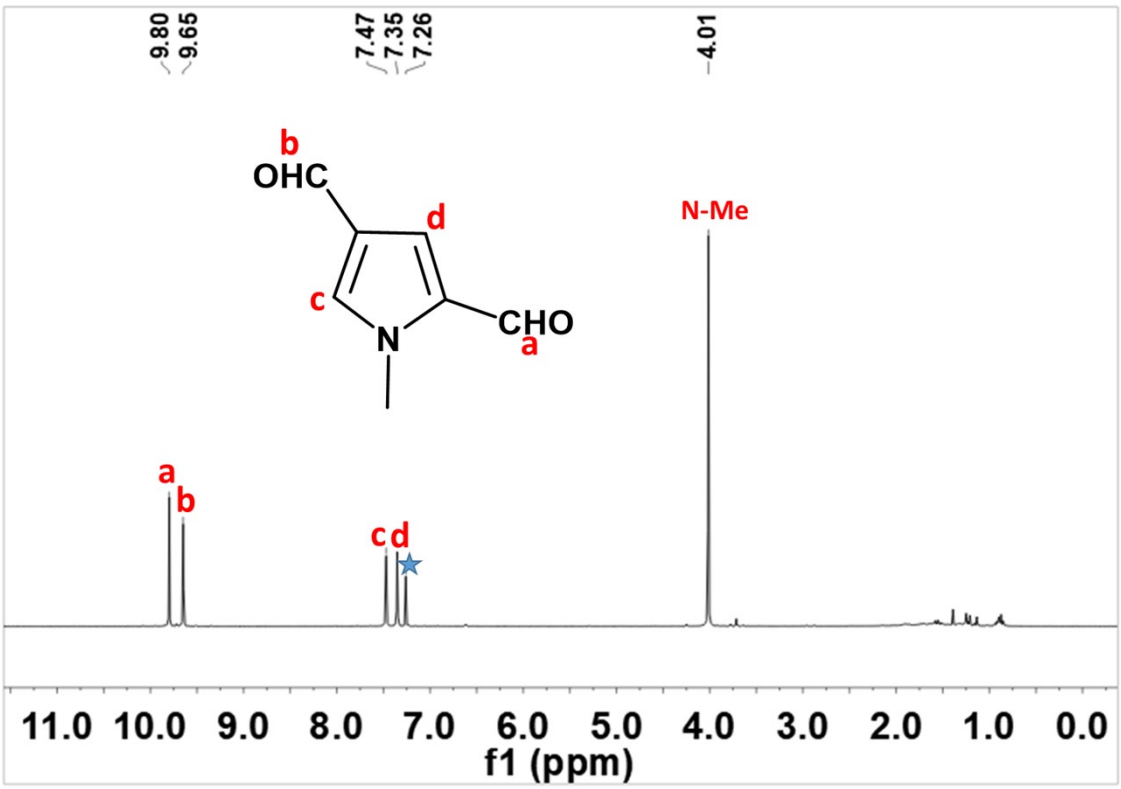

Fig. S8 ^{1}H NMR Spectra of **4** in $CDCl_3$.

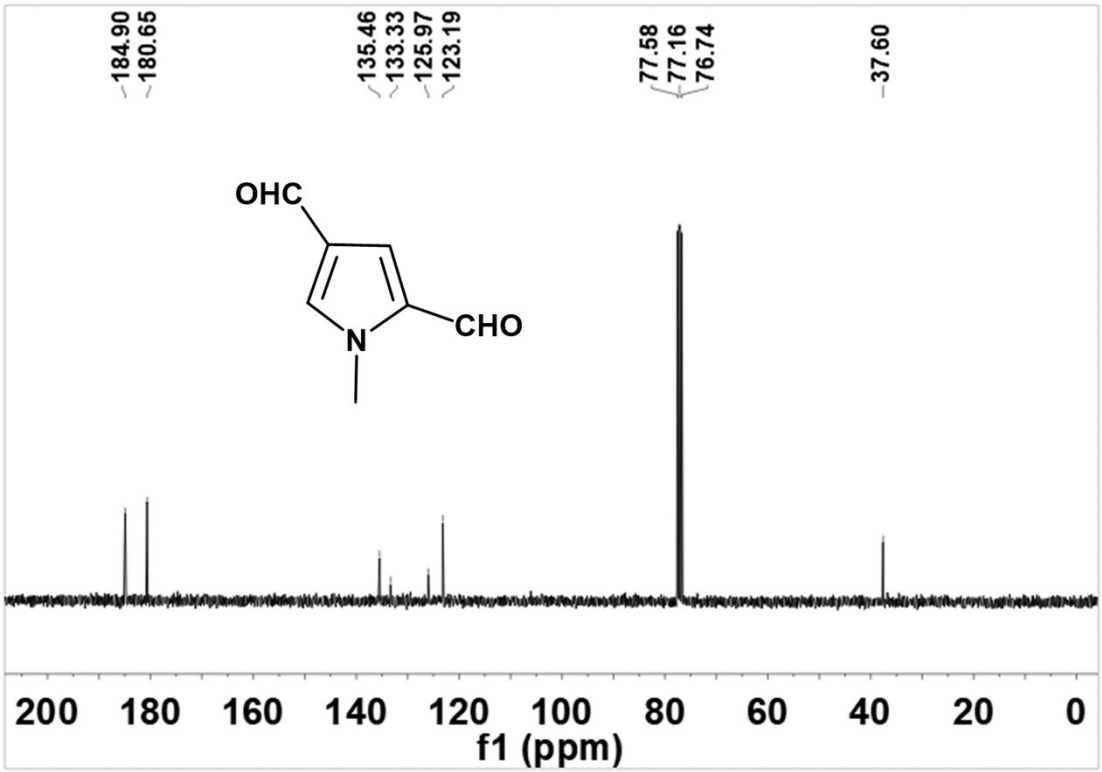

Fig. S9 ^{13}C NMR Spectra of **4** in $CDCl_3$.

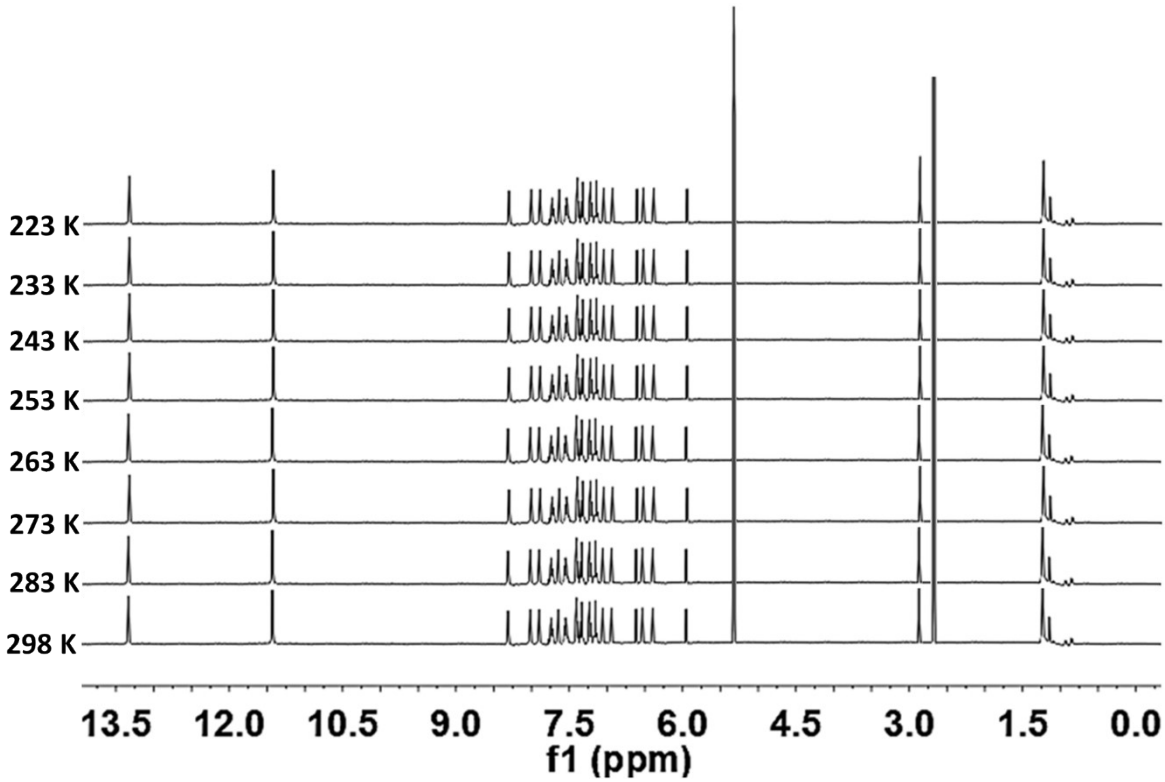

Fig. S10 Low VT ^{1}H NMR spectra of **5** in CD_2Cl_2.

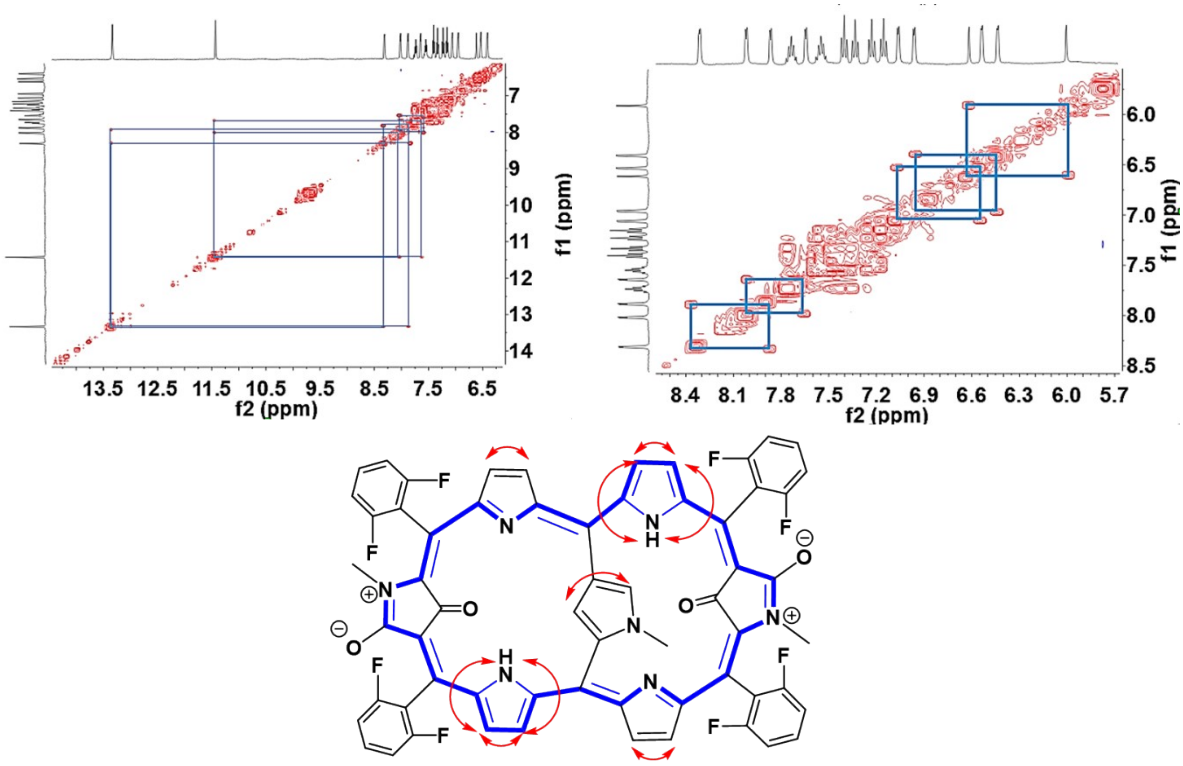

Fig. S11 ^{1}H-^{1}H 2D COSY NMR spectra of **5** in CD_2Cl_2 at 298 K.

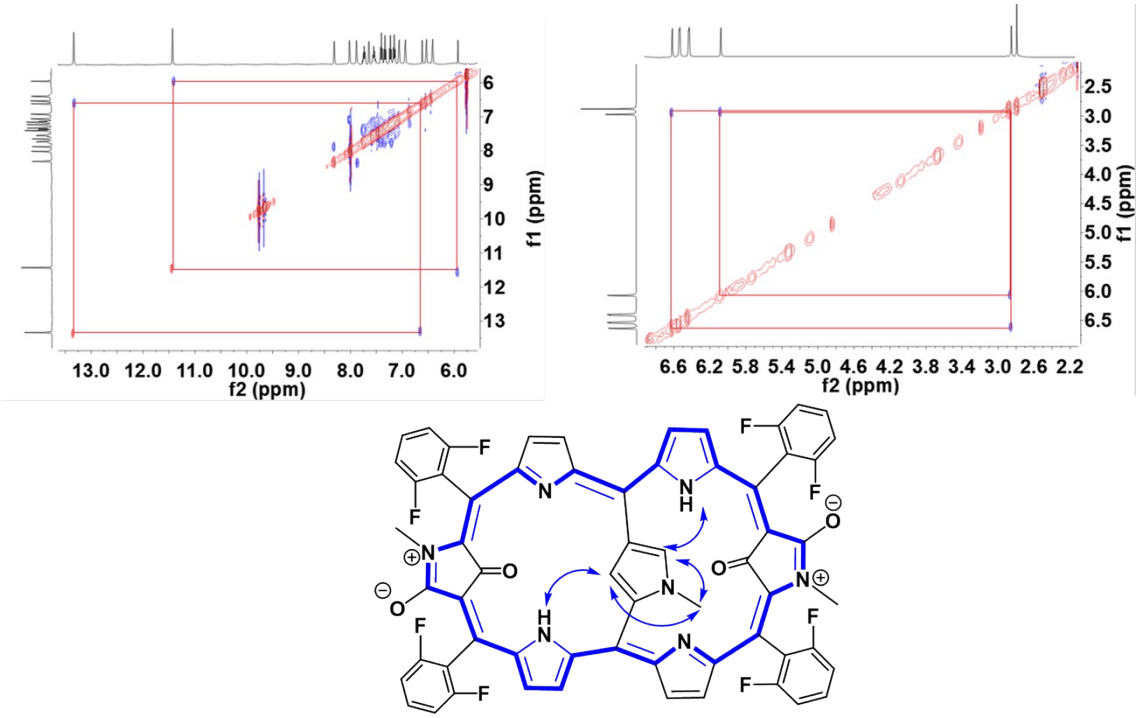

Fig. S12 ^{1}H-^{1}H 2D ROESY NMR spectra of **5** in CD_2Cl_2 at 298 K.

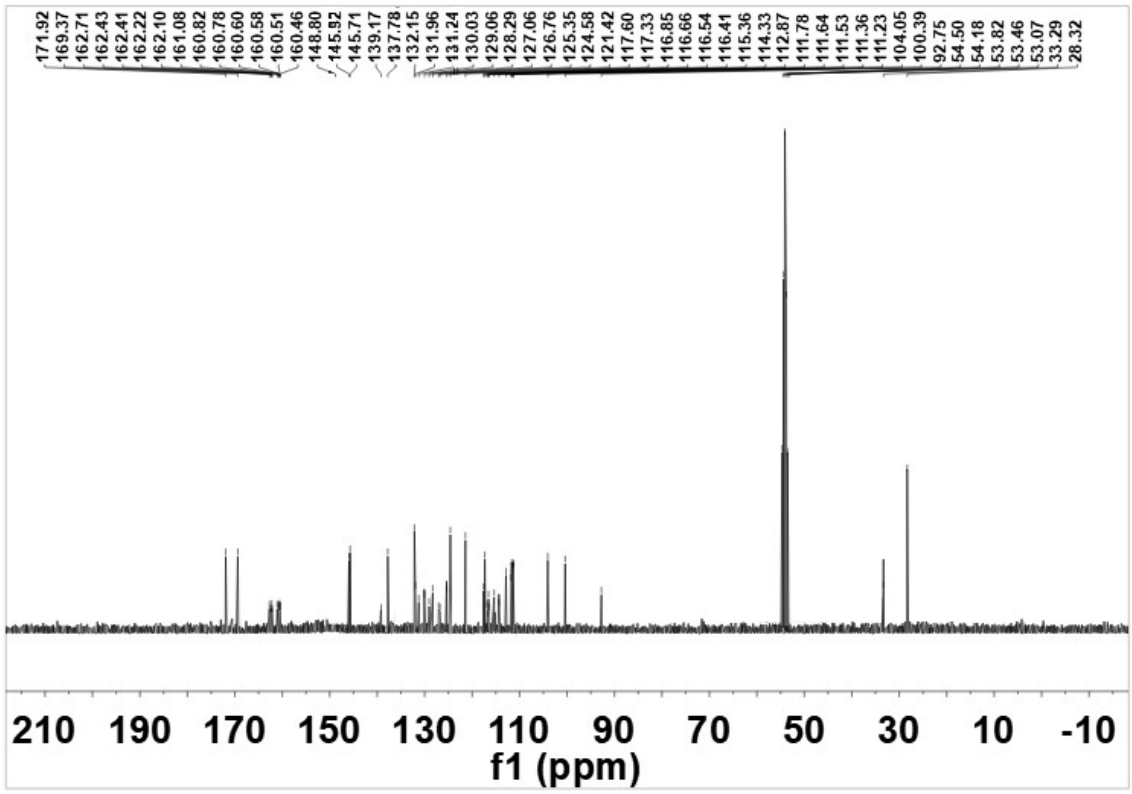

Fig. S13 ^{13}C NMR spectra of **5** in CD_2Cl_2 at 298 K.

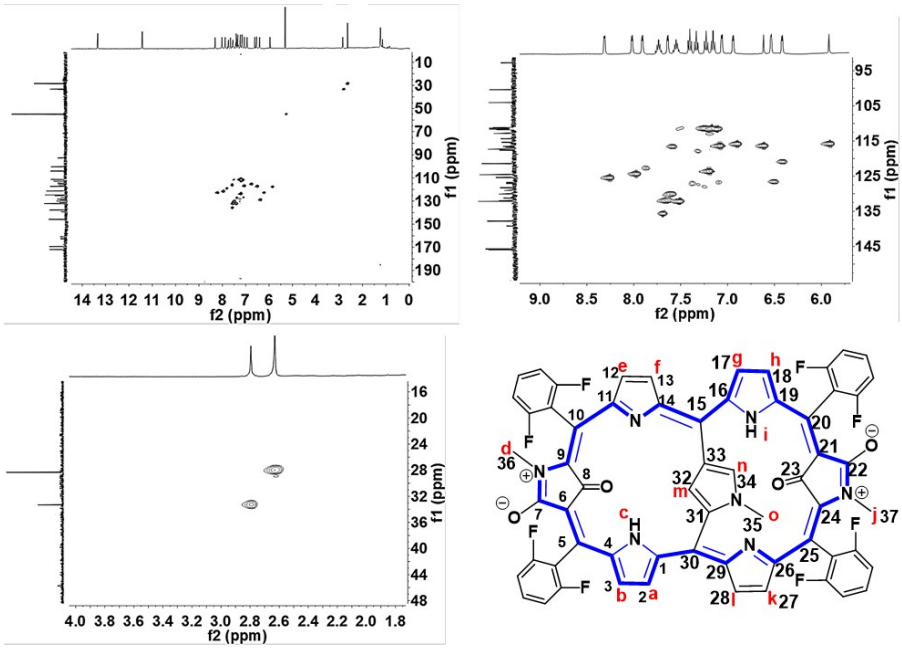

^{1}H (ppm)	^{13}C (ppm)	^{1}H (ppm)	^{13}C (ppm)
13.34(c)	-----	6.69(k)	115.4
11.43(i)	-----	6.62(m)	116.4
8.31(b)	126.7	6.54(f)	126.8
8.01(h)	125.3	6.40(l)	121.4
7.90(a)	124.5	5.95(n)	116.8
7.62(g)	116.7	2.87(o)	33.29
7.06(e)	116.5	2.64(d,j)	28.32

Fig. S14 ^{13}C-^{1}H 2D HSQC NMR spectra of **5** in CD_2Cl_2 at 298 K.

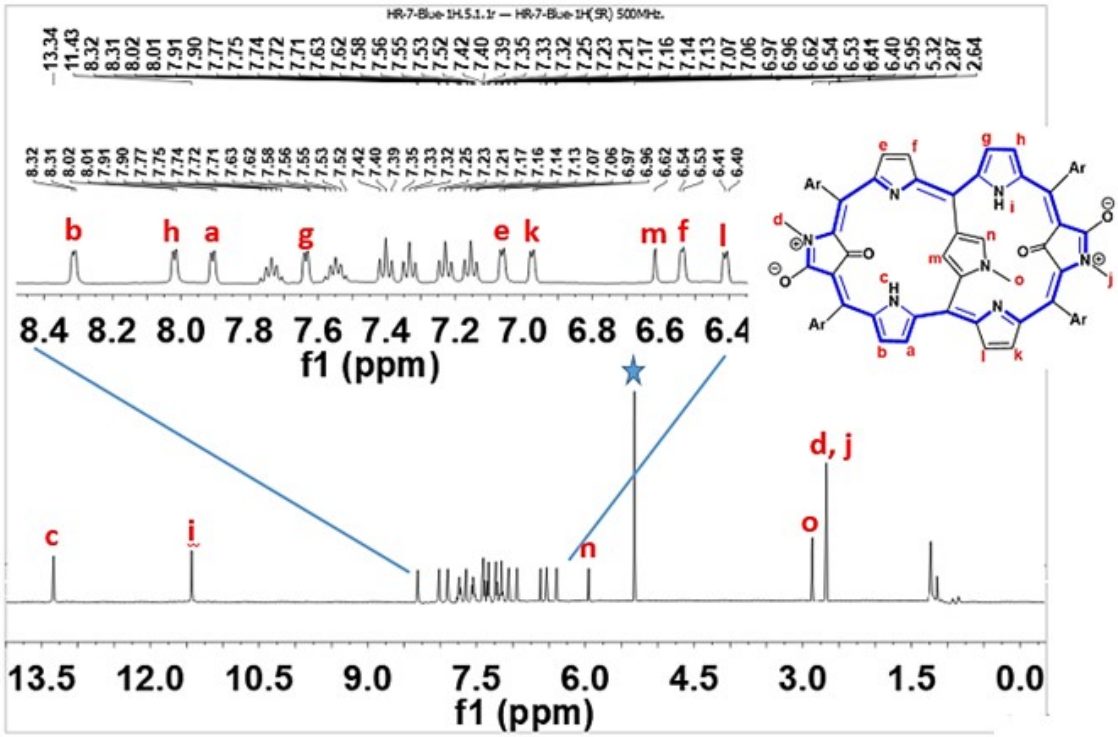

Fig. S15 Completely assigned ^{1}H NMR spectra of **5** in CD_2Cl_2 at 298 K.

4. DFT Calculations

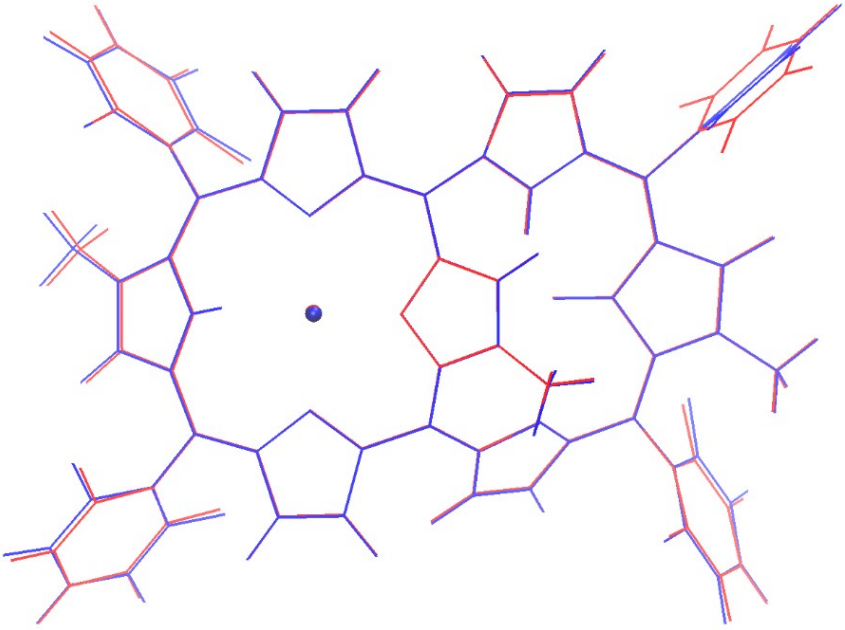

Fig. S16 Superimposition of the optimized structures of molecule **6** with the def2-TZVP (red) and def2-SVP (blue) basis sets.

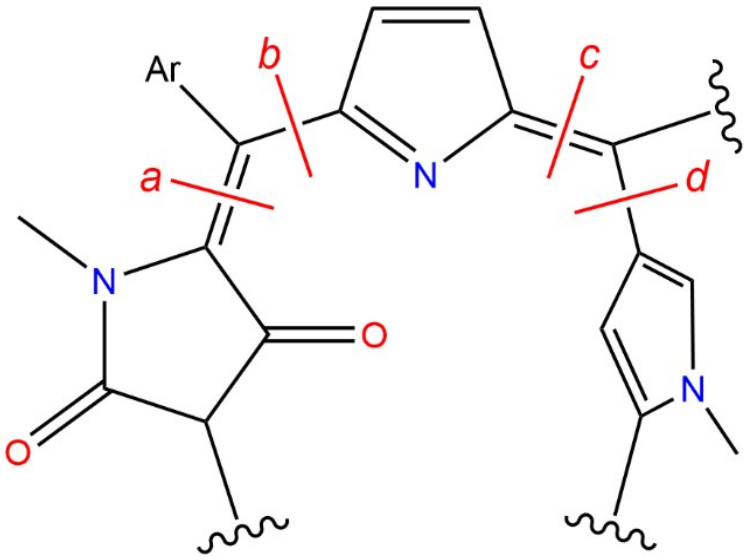

Fig. S17 Selected cut planes for the calculation of magnetically induced current density of **5** and **6** (Ar = 2,6-difluorophenyl). The Cu (II) atom of **6** (not shown) occupies the center of the considered macrocycle

Table S1. The strength (in nA T^{-1}) of the magnetically induced current density of **5** and **6** that pass through the integration planes shown in Figure S17

Plane	**5**	**6**
a	−2.51	−1.96
b	−1.29	-[a]
c	+0.19	−1.55
d	+0.21	-[a]

[a] The MIC strength value is perturbed by the close presence of other atoms to the integration plane.

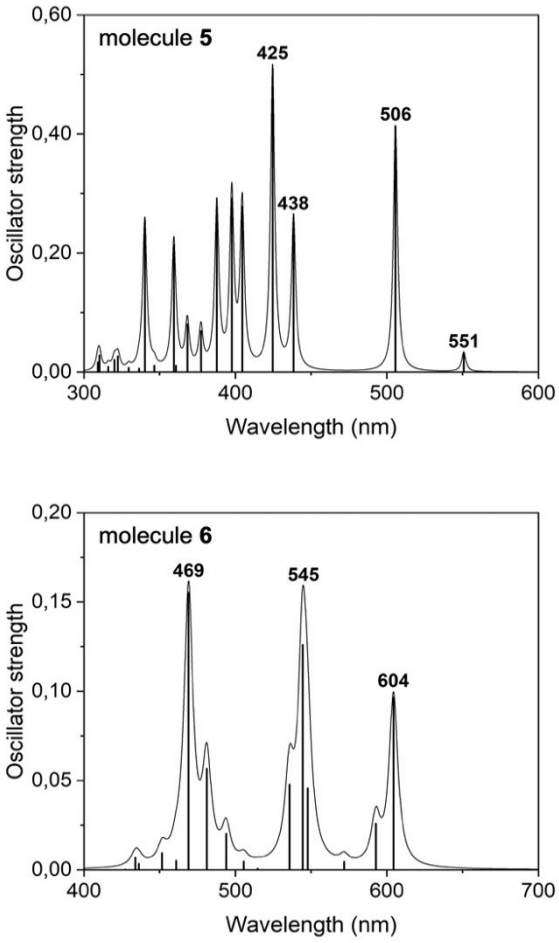

Fig. S18 Simulated UV-vis spectra of **5** (top) and **6** (bottom) calculated at RD-DFT/CAM-B3LYP level of Theory

Table S2. Energies (in nm), oscillator strengths (dimensionless), and orbital contributions (in %) of selected vertical singlet excitations of molecule **5**

Excitation	Energy	Oscillator strength	Contributions (%)	
$S_1 \leftarrow S_0$	551	0.03	275 $\rightarrow$ 277	(56.3)
			276 $\rightarrow$ 278	(17.5)
			276 $\rightarrow$ 277	(12.7)
$S_2 \leftarrow S_0$	506	0.41	276 $\rightarrow$ 277	(62.0)
			274 $\rightarrow$ 277	(14.5)
			275 $\rightarrow$ 277	(10.9)
$S_3 \leftarrow S_0$	438	0.26	274 $\rightarrow$ 277	(39.4)
			276 $\rightarrow$ 278	(17.9)
$S_4 \leftarrow S_0$	425	0.51	276 $\rightarrow$ 278	(47.9)
			274 $\rightarrow$ 277	(21.5)
			275 $\rightarrow$ 277	(14.6)

Table S3. Energies (in nm), oscillator strengths (dimensionless), and orbital contributions (in %) of selected vertical doublet excitations of molecule **6**

Excitation	Energy	Oscillator strength	Contributions (%)	
$D_5 \leftarrow D_0$	604	0.10	290α $\rightarrow$ 291α	(22.2)
			289β $\rightarrow$ 290β	(17.9)
			288β $\rightarrow$ 290β	(14.9)
			289α $\rightarrow$ 291α	(11.8)
$D_9 \leftarrow D_0$	545	0.13	289β $\rightarrow$ 290β	(14.2)
			288β $\rightarrow$ 290β	(13.3)
$D_{15} \leftarrow D_0$	469	0.16	287α $\rightarrow$ 291α	(16.6)
			286α $\rightarrow$ 291α	(12.1)

$S_1 \leftarrow S_0$ (551 nm)

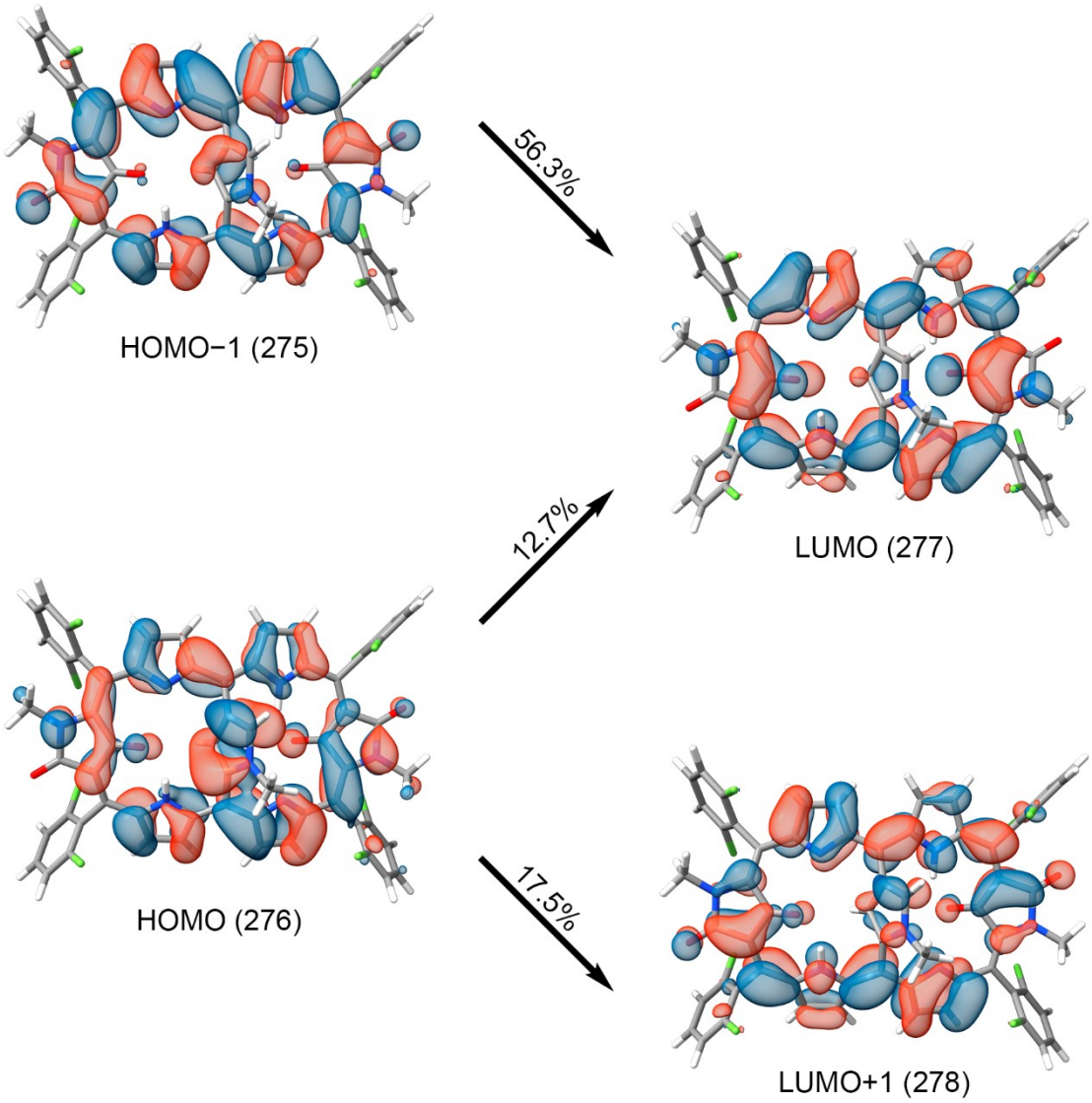

Fig. S19 Molecular orbitals involved in the $S_1 \leftarrow S_0$ transition of molecule **5**.

$S_2 \leftarrow S_0$ (506 nm)

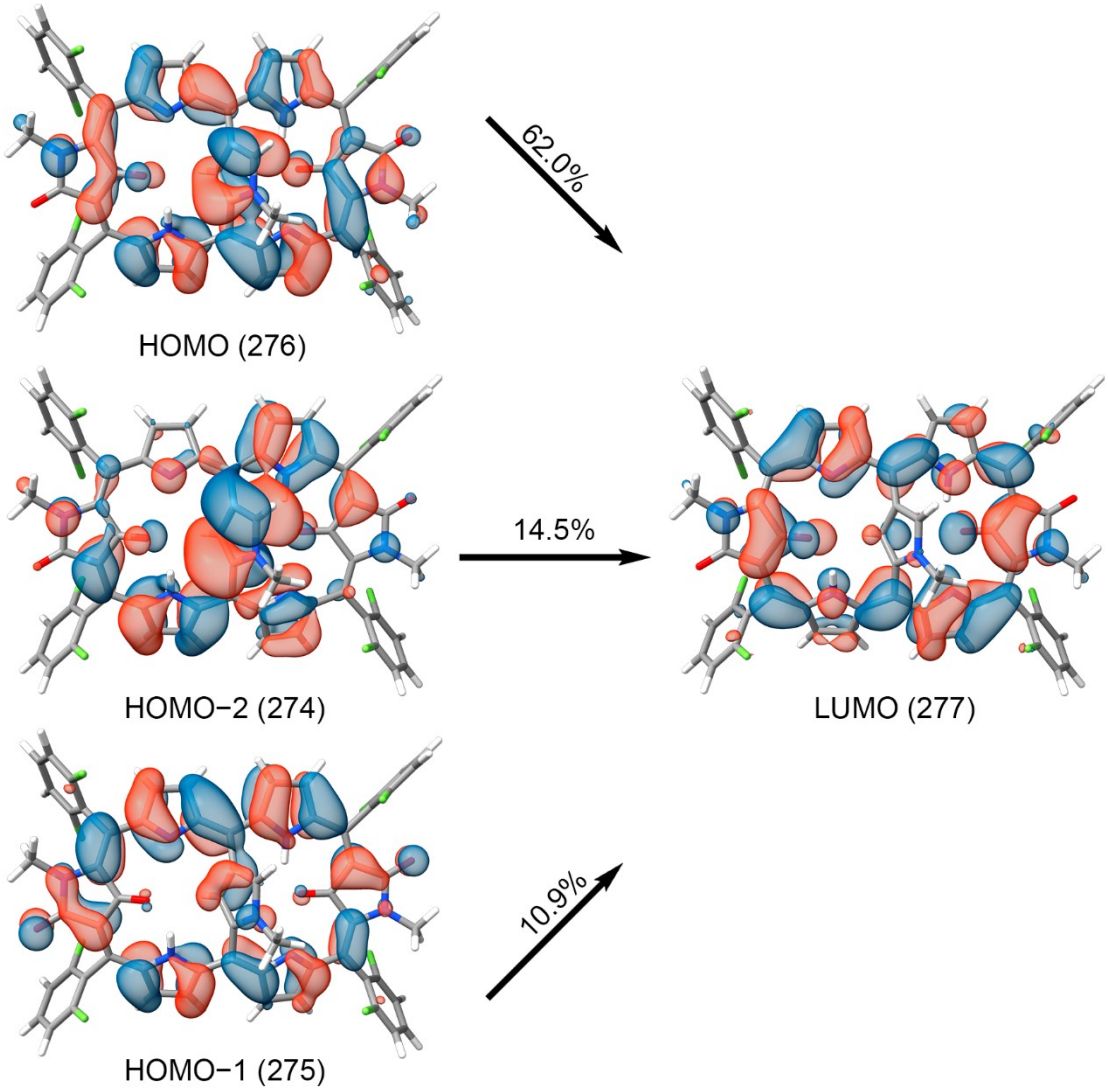

Fig. S20 Molecular orbitals involved in the $S_2 \leftarrow S_0$ transition of molecule **5**.

$S_3 \leftarrow S_0$ (438 nm)

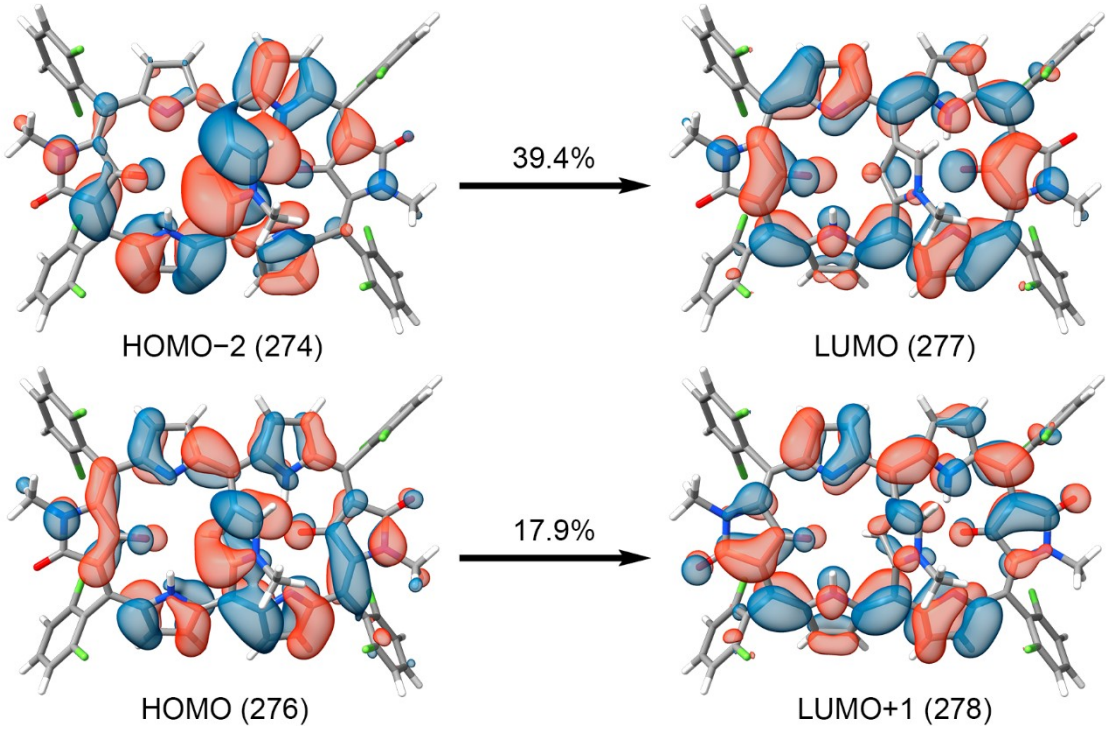

Fig. S21 Molecular orbitals involved in the $S_3 \leftarrow S_0$ transition of molecule **5**.

$S_4 \leftarrow S_0$ (425 nm)

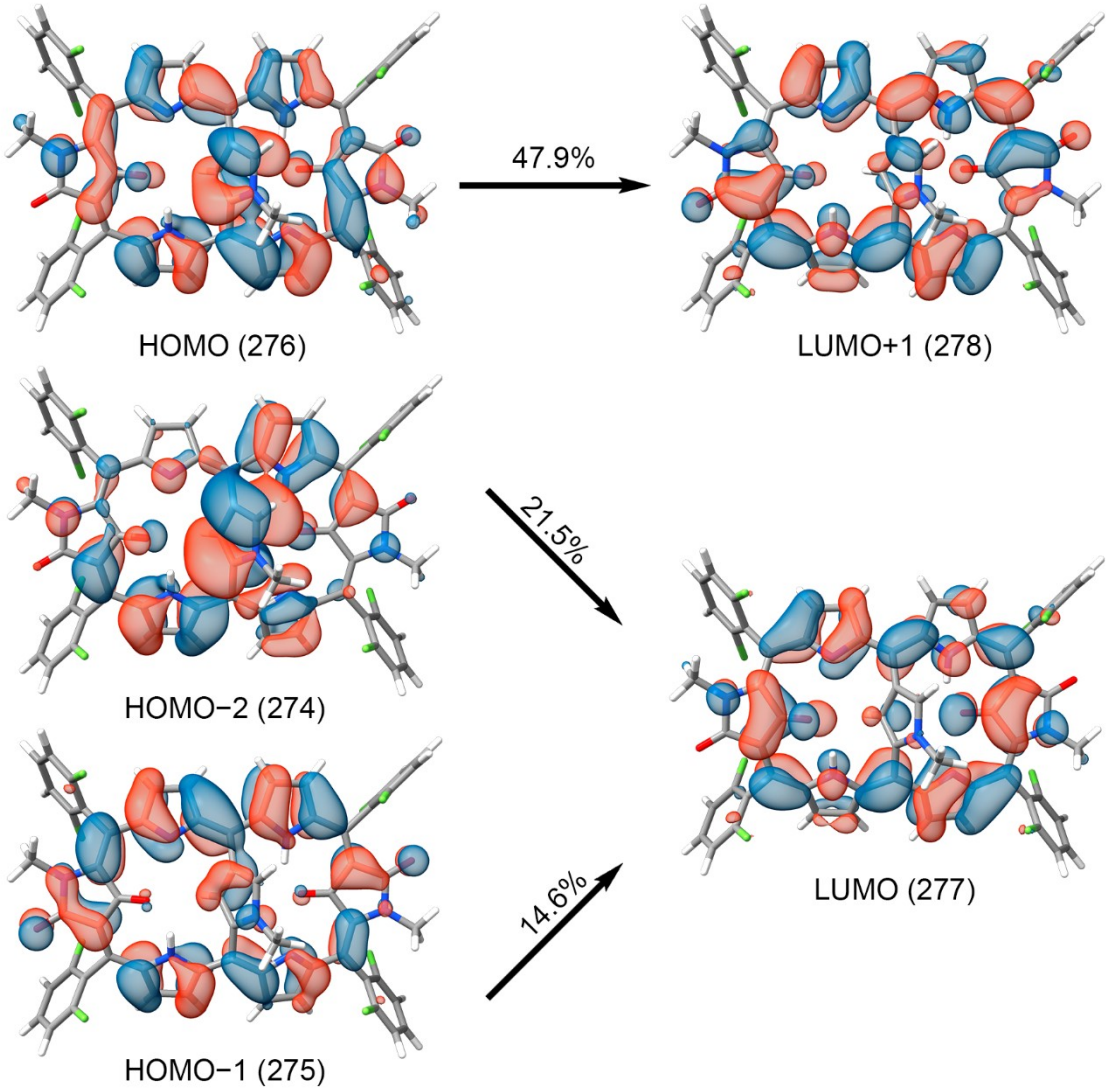

Fig. S22 Molecular orbitals involved in the $S_4 \leftarrow S_0$ transition of molecule **5**.

$D_5 \leftarrow D_0$ (604 nm)

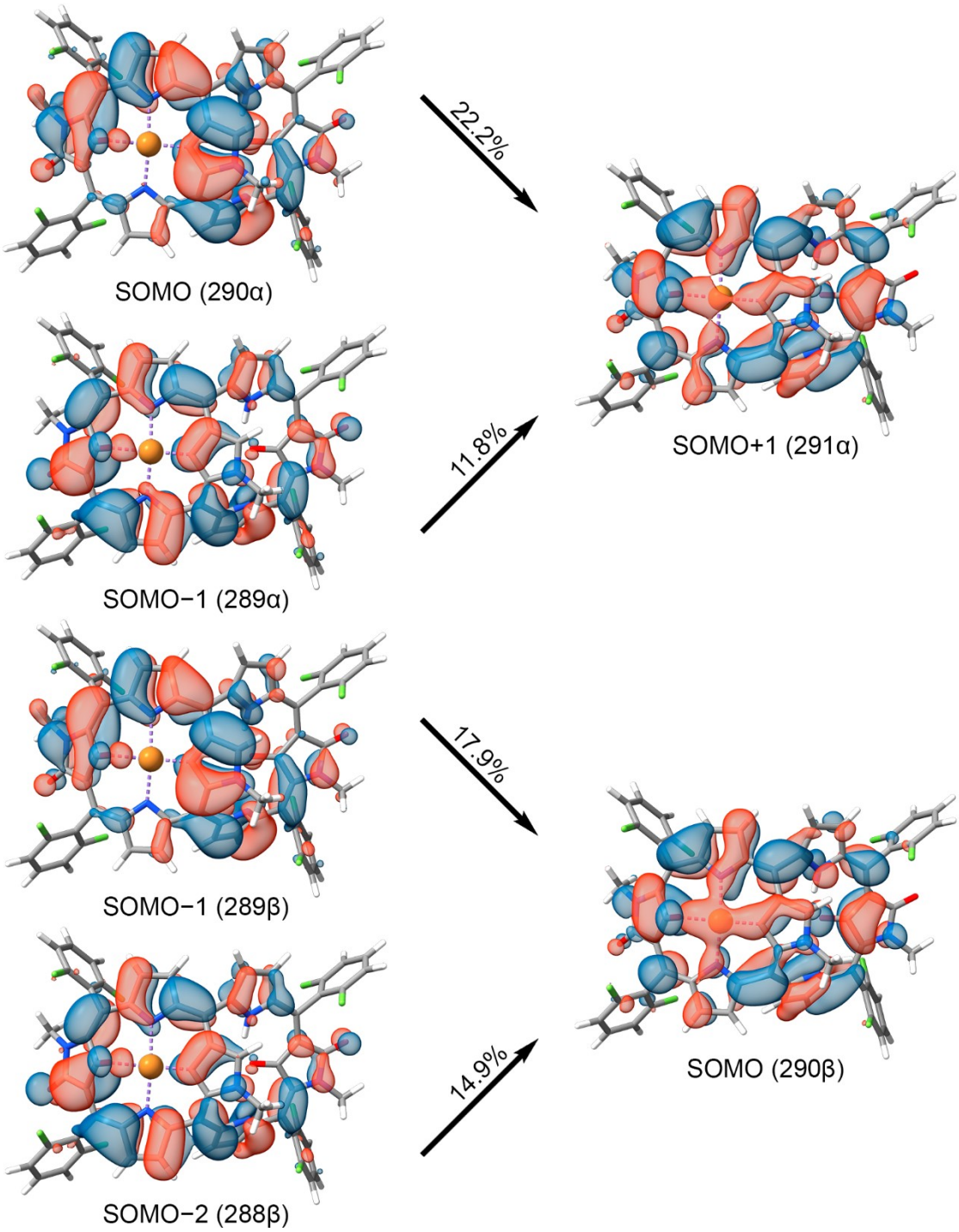

Fig. S23 Molecular orbitals involved in the $D_5 \leftarrow D_0$ transition of molecule **6**.

$D_9 \leftarrow D_0$ (545 nm)

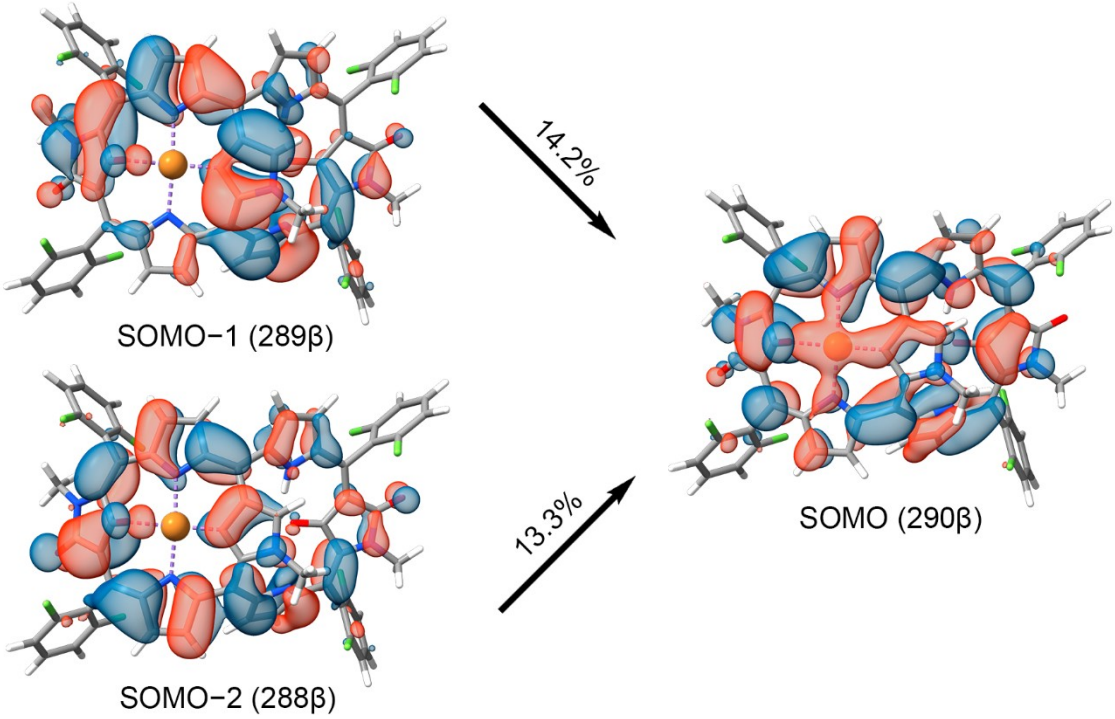

Fig. S24 Molecular orbitals involved in the $D_9 \leftarrow D_0$ transition of molecule **6**.

$D_{15} \leftarrow D_0$ (469 nm)

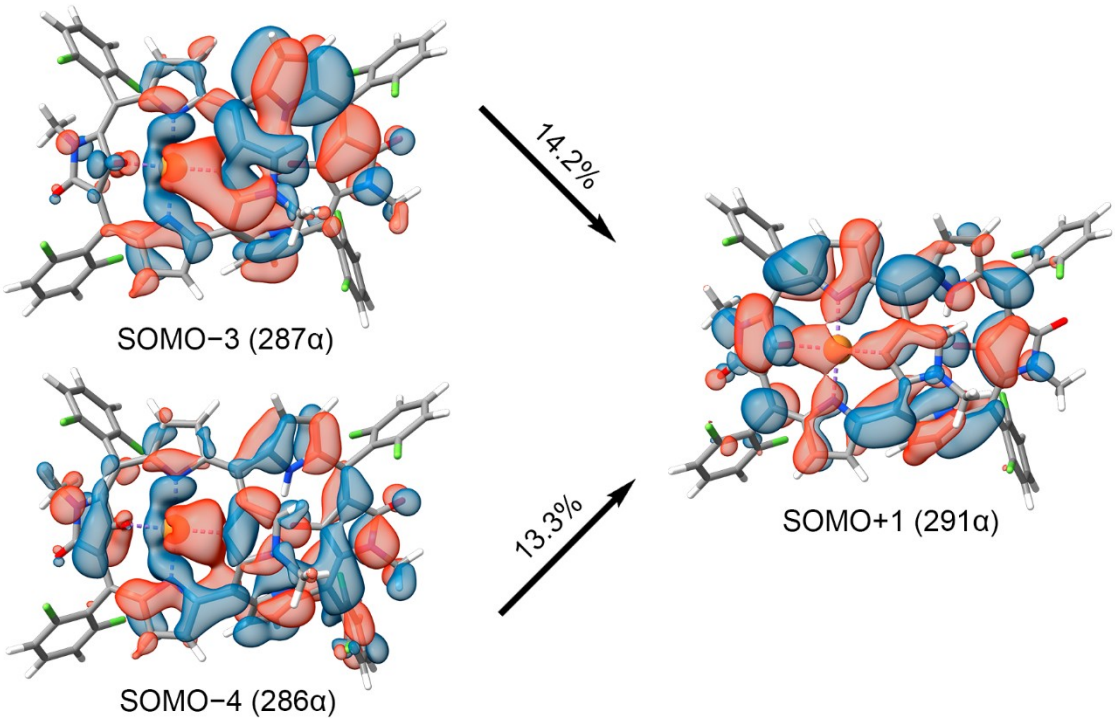

Fig. S25 Molecular orbitals involved in the $D_{15} \leftarrow D_0$ transition of molecule **6**.

5. Cartesian Coordinates

Cartesian coordinates of **5**

113

N	-6.4459355	0.9852097	1.2313257
C	-6.5880866	-0.3711019	0.9794843
C	-5.1081647	1.4002874	1.2225027
C	-4.3294625	0.1152955	1.3568437
C	-5.2286357	-0.9400021	0.8668982
C	-4.6736879	2.6544303	0.9766881
C	-3.2773090	3.0808192	0.8496261
C	-4.9360537	-2.1645719	0.3626523
C	-3.6378323	-2.7405504	0.1547188
N	-2.4614471	-2.2455122	0.6235345
C	-1.4089095	-2.9321020	0.1091216
C	-1.9389281	-3.9278939	-0.7155170
C	-3.3199147	-3.8172619	-0.6764169
N	-2.2520122	2.3440313	1.1344190
C	-1.1192693	3.0576211	0.7724334
C	-2.8592390	4.3763378	0.2940152
C	-1.5148776	4.3535741	0.2513600
C	-5.6541241	3.7117018	0.6122442
C	-5.9315734	4.7870186	1.4386256
C	-6.2956320	3.7183870	-0.6149701
C	-7.1663331	4.7107031	-1.0097047
C	-7.4124364	5.7572784	-0.1395198
C	-6.7946849	5.8041458	1.0983217
C	-6.0490953	-3.0106491	-0.1475811
C	-6.4626993	-4.1426184	0.5284464
C	-6.7147276	-2.7255824	-1.3252679
C	-7.4770902	-4.9579488	0.0799386
C	-7.7294699	-3.5095457	-1.8223469
C	-8.1084503	-4.6312871	-1.1064239
C	0.0959578	2.4592020	0.8584606
C	0.1899101	1.0413104	1.1979386
C	-0.0578168	-2.5077561	0.4094804
C	0.0649517	-1.1913180	1.0307897
C	-0.4283303	-0.0188813	0.5147690
C	1.0119290	0.4702637	2.1460288
N	0.9188747	-0.8730921	2.0569236
O	-3.2474313	-0.0279592	1.8668371
O	-7.6574375	-0.9294876	0.9260572
C	1.6201175	-1.7961748	2.9213873
C	-7.6053904	1.7597759	1.6180860
F	-5.3365163	4.8238026	2.6382264
F	-6.0636013	2.7014819	-1.4543333
F	-5.8516527	-4.4457438	1.6819745
F	-6.3492209	-1.6327879	-2.0082033
H	-6.9707392	6.6084179	1.7974671
H	-8.0932862	6.5455129	-0.4285338
H	-7.6342977	4.6499134	-1.9812881
H	-7.3331561	2.4548565	2.4086607
H	-8.0362597	2.3136982	0.7859767
H	-8.3500657	1.0576494	1.9833979
H	-7.7587971	-5.8232813	0.6615106
H	-8.9084764	-5.2569096	-1.4765534
H	-8.2105116	-3.2296354	-2.7478468
H	-4.0288682	-4.4161442	-1.2207626
H	-1.3814905	-4.6269305	-1.3087142
H	-0.8585428	5.1163368	-0.1327823
H	-3.5044488	5.1743416	-0.0345711
C	1.3655619	3.0742522	0.5229203
C	1.0862844	-3.1273379	-0.0090073
N	2.2977463	-2.4514635	0.1096363
C	3.1560604	-3.0702085	-0.6343798
C	2.5744378	-4.2776962	-1.2235018
C	1.2936587	-4.3178967	-0.8147551
C	1.8814331	4.3727885	0.5873677
C	3.2074454	4.3104951	0.1819898
C	3.4972149	2.9745239	-0.1333243
N	2.3547507	2.2717674	0.0844904
C	4.7504531	2.3736175	-0.4426737
C	5.0134704	1.0429318	-0.6275285
C	4.1059275	-0.0934578	-0.7847753
C	4.9553971	-1.3438221	-0.7728132
C	4.5379276	-2.6285043	-0.8426107
C	6.3770381	0.4892065	-0.6703106
N	6.2706571	-0.8979242	-0.7429830
C	5.8807602	3.3413945	-0.4849481
C	6.3906550	3.8095250	-1.6804899
C	7.4187699	4.7210343	-1.7516441
C	7.9730780	5.1837370	-0.5717191
C	7.5006371	4.7419056	0.6512223
C	6.4668584	3.8342515	0.6647747
F	5.8549097	3.3466754	-2.8178202
F	6.0136178	3.3859240	1.8445288
C	5.4592867	-3.7361413	-1.1941525
C	6.0868429	-3.8109838	-2.4278587
F	5.9220026	-2.7943427	-3.2846343
C	6.8765042	-4.8711294	-2.8166678
C	7.0569649	-5.9196528	-1.9334980
C	6.4541189	-5.9006595	-0.6873337
C	5.6716625	-4.8192929	-0.3537040
F	5.0996354	-4.7938690	0.8573508
O	2.9163432	-0.0657357	-1.0080658
O	7.4379224	1.0626266	-0.6012813
C	7.4551808	-1.6917598	-0.5025496
H	-2.4163876	-1.4453801	1.2551308
H	2.2540054	1.2948999	-0.1943459
H	1.3536183	5.2404478	0.9427388
H	3.9103280	5.1249624	0.1536019
H	0.5680875	-5.0741355	-1.0530325
H	3.0749665	-4.9804337	-1.8696689
H	6.5821641	-6.7030791	0.0242635
H	7.6746468	-6.7599262	-2.2176228
H	7.3341947	-4.8595505	-3.7949792
H	8.2337957	-1.0064388	-0.1815148
H	7.7942727	-2.2042401	-1.4002787
H	7.2635353	-2.4254905	0.2777629
H	7.7727210	5.0466582	-2.7186291
H	8.7858781	5.8955033	-0.6055837
H	7.9227599	5.0801193	1.5860109
H	-1.0951456	0.0735358	-0.3236223
H	1.6190614	0.9360018	2.9039873
H	1.7097938	-1.3529853	3.9108679
H	1.0545540	-2.7204496	3.0038052
H	2.6026141	-2.0254728	2.5160230

Cartesian coordinates of **6**
112

N	4.3836310	1.4711650	0.4652860
C	4.5315270	0.0658600	0.4667260
C	3.1171230	1.8315210	0.0388230
C	2.5541790	0.5866590	-0.5560730
C	3.2969790	-0.5010640	-0.0780820
C	2.4349670	2.9847010	0.2184330
C	0.9865060	3.2126070	0.0779060
C	2.9322040	-1.8487890	-0.0755670
C	1.6362870	-2.3603990	-0.1052660
N	0.4476510	-1.6462240	0.0366600
C	-0.5173360	-2.5439890	0.2369970
C	-0.0063530	-3.8659190	0.1673680
C	1.3320960	-3.7496840	-0.0524860
N	-0.0059950	2.3316170	-0.0474330
C	-1.2018490	3.0263660	0.1378110
C	0.4423830	4.5282400	0.2919890
C	-0.9008400	4.3998620	0.3750160
C	3.1505190	4.1683050	0.7715930
C	3.9107830	5.0075940	-0.0229360
C	3.0630620	4.5242330	2.1075100
C	3.6896660	5.6262880	2.6424990
C	4.4411690	6.4293380	1.8012800
C	4.5574170	6.1264220	0.4570480
C	4.0322310	-2.8323630	0.0937450
C	4.9582070	-3.0557190	-0.9107890
C	4.2292440	-3.5378290	1.2680600
C	6.0034710	-3.9411290	-0.7888960
C	5.2654230	-4.4264190	1.4462590
C	6.1516140	-4.6262070	0.4038470
C	-2.4650200	2.4754820	0.1253160
C	-2.7532510	1.1247390	-0.2112820
C	-1.9271540	-2.2230780	0.5221930
C	-2.5066130	-1.0833670	-0.1441980
C	-1.8045740	0.0850410	-0.1869680
C	-4.0140240	0.5244750	-0.3319210
N	-3.8646400	-0.7976230	-0.2947360
O	1.6384180	0.5907870	-1.3930650
O	5.5221410	-0.4834950	0.8814730
C	-4.9326080	-1.7462650	-0.5414100
C	5.4124320	2.2790360	1.0788600
F	4.0327860	4.7091900	-1.3230080
F	2.3432280	3.7386890	2.9181410
F	4.8178010	-2.3813770	-2.0588680
F	3.3895400	-3.3241100	2.2892270
H	5.1380880	6.7354180	-0.2201610
H	4.9423190	7.3004820	2.1993070
H	3.5854910	5.8383180	3.6964530
H	5.7072010	3.0962720	0.4256780
H	5.0982380	2.6805870	2.0410200
H	6.2627600	1.6217990	1.2356520
H	6.6845650	-4.0743150	-1.6163580
H	6.9715720	-5.3203070	0.5240320
H	5.3684380	-4.9358970	2.3929500
H	2.0457840	-4.5482390	-0.1604800
H	-0.5896480	-4.7660910	0.2573320
H	-1.6243930	5.1755950	0.5579740
H	1.0107440	5.4347200	0.3968790
C	-3.6045520	3.1568170	0.7646220
C	-2.5600720	-2.7993760	1.5891320
N	-3.8072110	-2.3420150	2.0040100
C	-3.9631650	-2.7347970	3.2280970
C	-2.8515380	-3.5664090	3.6743330
C	-1.9811440	-3.6112470	2.6480320
C	-4.3172110	4.3479120	0.6383640
C	-5.3726180	4.2935570	1.5489980
C	-5.2883140	3.0714410	2.2280470
N	-4.1983130	2.4329100	1.7268520
C	-6.2028900	2.4406780	3.1169980
C	-6.1569190	1.1515180	3.5835410
C	-5.1356870	0.1094660	3.4473020
C	-5.7174660	-1.1602450	4.0094910
C	-5.1243640	-2.3735080	4.0500120
C	-7.2662190	0.5330390	4.3359240
N	-6.9444960	-0.8033270	4.5508030
C	-7.3613380	3.3028050	3.4799040
C	-7.3740110	4.0518120	4.6396610
C	-8.4183810	4.8782110	4.9859410
C	-9.5054100	4.9594230	4.1343580
C	-9.5394340	4.2282050	2.9600710
C	-8.4675720	3.4196030	2.6618730
F	-6.3195990	3.9564900	5.4607510
F	-8.4942320	2.6931200	1.5339170
C	-5.5553340	-3.4426270	4.9778630
C	-5.5599120	-3.2698580	6.3543710
F	-5.2535610	-2.0597180	6.8418370
C	-5.8640410	-4.2741160	7.2468120
C	-6.1831490	-5.5247800	6.7508020
C	-6.1940950	-5.7577220	5.3863150
C	-5.8775080	-4.7203510	4.5399040
F	-5.9051540	-4.9428080	3.2201530
O	-3.9857960	0.2207340	3.0741130
O	-8.3114440	1.0222490	4.6923590
C	-7.9715620	-1.7016060	5.0270190
H	-3.8641240	1.5436960	2.1173560
H	-4.1137100	5.1337130	-0.0683980
H	-6.1446560	5.0318730	1.6807280